Theoretical Analysis and Synthesis of Switching Table for Direct-Power-Controlled PWM Converter

Nguyen Van Hung, and Toshihiko Noguchi (Nagaoka University of Technology)

I. Introduction

This paper describes theoretical analysis and synthesis of the switching table for a direct-power-controlled three-phase PWM converter. This analysis gives a theoretical basis to compose the switching table of the converter, which had been conventionally determined by a trial-and-error method through computer simulations.

II. Control System Configuration

A block diagram of the control system is depicted in Fig. 1, where the resistances of the interconnecting reactors are neglected [1], [2]. The phase of the source voltage space vector is converted to the digitized signals, i.e. θ_n ($\because n$=1~12), by using several comparators. Fig. 2 shows the quantized phase sectors and the controller detects one of the sectors where the power source voltage vector exists. Also, the active-power and the reactive-power errors are similarly converted to the digitized signals, i.e. S_p and S_q, by using hysteresis comparators. If S_p or S_q=1, P or Q increases, while S_p or S_q=0, P or Q decreases. The digitized error signals S_p, S_q, and θ_n are given to the switching table, in which the switching states S_a, S_b and S_c of the converter are stored as shown in TABLE I or II.

III. Theoretical Analysis

Because the values S_p and S_q are either 1 or 0 corresponding to increase or decrease of P and Q, the polarities of dP/dt and dQ/dt are the most important factors to determine the switching modes of the converter. Therefore, it is indispensable to examine mathematically dP/dt and dQ/dt under various combinations of the switching states S_a, S_b and S_c, and the power source voltage phase θ_n.

The power source voltage vector v_s can be expressed as follows:

$$v_S = \sqrt{2/3}\left(v_a + v_b e^{j2\pi/3} + v_c e^{j4\pi/3}\right), \quad \cdots\cdots (1)$$

$$\text{where } \left.\begin{aligned} v_a &= \sqrt{2}V_{rms}\cos\omega t \\ v_b &= \sqrt{2}V_{rms}\cos(\omega t - 2\pi/3) \\ v_c &= \sqrt{2}V_{rms}\cos(\omega t - 4\pi/3) \end{aligned}\right\}. \quad \cdots\cdots (2)$$

Substituting (2) into (1), the voltage vector v_s can be obtained as

$$v_S = \sqrt{3}V_{rms}e^{j\omega t}. \quad \cdots\cdots (3)$$

The converter output voltage vector v_c is expressed as

$$v_C = \sqrt{2/3}V_{dc}\left(S_a + S_b e^{j2\pi/3} + S_c e^{j4\pi/3}\right). \quad \cdots\cdots (4)$$

And the voltage and current equation with respect to the reactor is expressed as (5):

$$v_S - v_C = L\,di/dt. \quad \cdots\cdots (5)$$

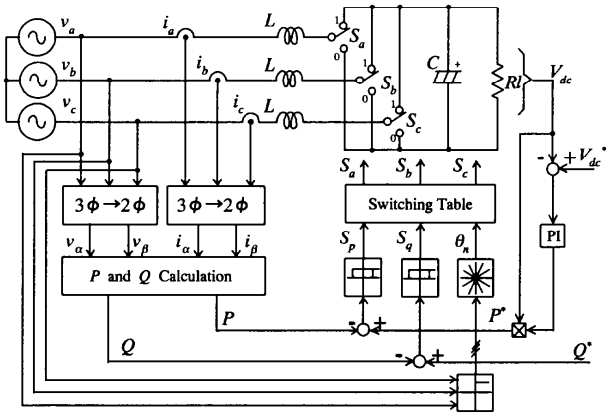

Fig. 1. Block diagram of direct-power-controlled PWM converter.

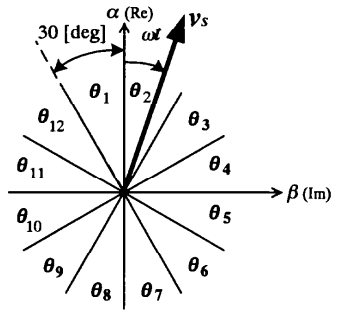

Fig. 2. Power source voltage vector and phase sectors.

Table I Conventional switching table

S_p	S_q	θ_1	θ_2	θ_3	θ_4	θ_5	θ_6	θ_7	θ_8	θ_9	θ_{10}	θ_{11}	θ_{12}
1	0												
1	1	111	111	000	000	111	111	000	000	111	111	000	000
0	0	101	100	100	110	110	010	010	011	011	001	001	101
0	1	100	110	110	010	010	011	011	001	001	101	101	100

Table II Novel switching table

S_p	S_q	θ_1	θ_2	θ_3	θ_4	θ_5	θ_6	θ_7	θ_8	θ_9	θ_{10}	θ_{11}	θ_{12}
1	0												
1	1	111	111	000	000	111	111	000	000	111	111	000	000
0	0	101	100	100	110	110	010	010	011	011	001	001	101
0	1	100	110	110	010	010	011	011	001	001	101	101	100

Table III Conventional simulation result

Converter output voltage vector		Power source voltage vector position [ωt]				
		-30 [deg]	-15 [deg]	0 [deg]	15 [deg]	30 [deg]
111	P	↗	↗	↗	↗	↗
	Q	↗	↗	↗	↗	↗
101	P	↘	↗	↗	↗	↗
	Q	↘	↘	↘	↘	↘
100	P	↘	↘	↘	↘	↘
	Q	↗	↗	↗↘	↘	↘
110	P	↗	↗	↗	↘	↘
	Q	↗	↗	↗	↗	↗

The equations for instantaneous powers P and Q are

$$P = v_\alpha i_\alpha + v_\beta i_\beta \text{, and} \quad \cdots\cdots (6)$$

$$Q = v_\beta i_\alpha - v_\alpha i_\beta \text{,} \quad \cdots\cdots (7)$$

where $v_s = v_\alpha + jv_\beta$ and $i = i_\alpha + ji_\beta$. After solving the equations from (3) to (7), the equations of dP/dt and dQ/dt can be derived as (8) and (9), respectively.

$$dP/dt = \left(\sqrt{2}V_{rms}V_{dc}/L\right)\left[(S_a - S_b/2 - S_c/2)(\omega t \sin\omega t - \cos\omega t) - \sqrt{3}/2(S_b - S_c)(\omega t \cos\omega t + \sin\omega t)\right] \quad \cdots (8)$$

$$dQ/dt = \left(\sqrt{2}V_{rms}V_{dc}/L\right)\left[\sqrt{3}/2(S_b - S_c)(\cos\omega t - \omega t \sin\omega t) - (S_a - S_b/2 - S_c/2)(\sin\omega t - \omega t \cos\omega t)\right] \quad \cdots\cdots (9)$$

Therefore, it is possible to determine whether the dP/dt and dQ/dt are positive or negative according to every given combination of S_a, S_b, S_c and ωt.

IV. Synthesis of Switching Table

1. Conventional Method The conventional method was based on a trial-and-error approach using computer simulations and concrete gradients of P and Q with respect to every possible combination of S_a, S_b, S_c and ωt were examined. TABLE III shows an example of the simulation results.

2. Novel Method This method is based on the gradients of P and Q expressed theoretically by (8) and (9). If the polarities of dP/dt and dQ/dt are known by substituting S_a, S_b, S_c and ωt into (8) and (9), S_p and S_q can be determined to be either 1 or 0, respectively. The flowchart depicted in Fig. 3 shows how to find the optimum switching modes. The novel switching table obtained through this algorithm is shown in TABLE II.

V. Simulation System Configuration and Results

The system configuration of the simulation is identical to that of Fig. 1. The simulations were executed to compare the operating characteristics between the conventional-switching-table-based system and the novel-switching-table-based system. The simulation results are shown in Fig. 4 and Fig. 5. In both cases, the error signals of P and Q are properly controlled by the hysteresis comparators and restricted within the hysteresis bands of P and Q. In addition, the line current is in-phase with the line voltage, i.e. the unity power factor operation is successfully performed. However, in case of the conventional system, periodic ripples can be seen in the input current, which are caused by the ripples of Q. These ripples occur as a result of inappropriate selection of switching modes. On the other hand, the waveforms have been improved by the novel system and effectiveness of the novel switching table are confirmed.

VI. Conlusion

This paper has presented the theoretical analysis and synthesis of the switching table and has mathematically clarified dP/dt and dQ/dt. With this theoretical knowledge, the novel switching table has been created to optimize the waveforms of the powers, the currents and the voltages.

References

[1] T. Noguchi, H. Tomiki, S. Kondo, and I. Takahashi: *IEEE Trans. Ind. Appl.*, Vol. 34, No. 3, pp. 473- 479, 1998.

[2] T. Noguchi, H. Tomiki, S. Kondo, and S. Takahashi, and J. Katsumata: *IEEJ Trans. Ind. Appl.*, Vol. 116D, No. 2, pp. 222-223, 1996.

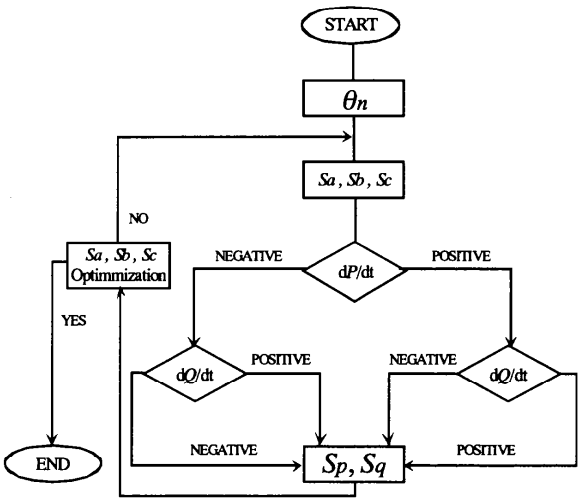

Fig. 3. Flowchart to compose novel switching table.

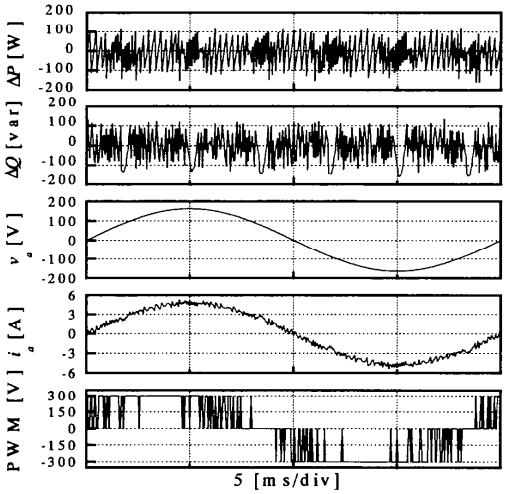

Fig. 4. Simulation result by conventional switching table.

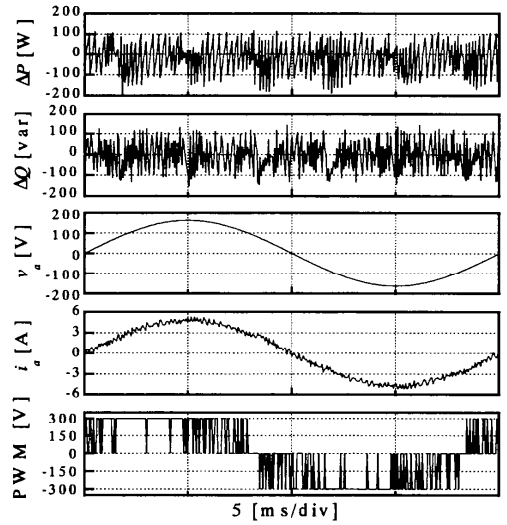

Fig. 5. Simulation result by novel switching table.